LATTICE BOLTZMANN SIMULATION OF TURBULENT NATURAL CONVECTION IN TALL ENCLOSURES

by

Hasan SAJJADI [a*] ***and Reza KEFAYATI*** [b]

[a] Department of Engineering, Shahid Bahonar University of Kerman, Kerman, Iran
[b] School of Computer Science, Engineering and Mathematics, Flinders University, Adelaide, Australia

Original scientific paper
DOI: 10.2298/TSCI120105066S

In this paper Lattice Boltzmann simulation of turbulent natural convection with large eddy simulations in tall enclosures which is filled by air with Pr = 0.71 has been studied. Calculations were performed for high Rayleigh numbers ($Ra = 10^7$-10^9) and aspect ratios change between 0.5 and 2 ($0.5 < AR < 2$). The present results are validated by finds of an experimental research at $Ra = 1.58 \cdot 10^9$. Effects of the aspect ratios in different Rayleigh numbers are displayed on streamlines, isotherm counters, vertical velocity and temperature at the middle of the cavity, local Nusselt number and average Nusselt number. The average Nusselt number increases with the augmentation of Rayleigh numbers. The increment of the aspect ratio causes heat transfer to decline in different Rayleigh numbers.

Key words: *lattice Boltzmann method, large eddy simulation, aspect ratio, natural convection*

Introduction

Turbulence in fluids is ubiquitous in nature and technological systems and represents one of the most challenging aspects in fluid mechanics. The difficulty stems from the inherent presence of many scales that are generally inseparable among many other factors. Nevertheless, considerable progress has been made over the years towards more fundamental physical understanding of turbulence phenomena through measurements, statistical phenomenological theories, modeling and computation [1, 2]. Also some experimental investigations have been done for instance Ampofo and Karayiannis [3] studied low-level turbulence natural convection in an air filled vertical square cavity while the hot and cold walls of the cavity were isothermal at 50 and 10 °C, respectively, giving a Rayleigh number of $Ra = 1.58 \cdot 10^9$.

Large eddy simulations (LES) provide a very promising approach for the simulation of turbulent flows because computation times are significantly lower than those of direct numerical simulations (DNS). Further, their resolution of turbulent structures is more accurate in comparison to Reynolds averaged Navier_Stokes (RANS) simulations [4-8].

The lattice Boltzmann method (LBM) is a computational alternative for simulating fluid flows and is rapidly gaining attention. It is an attractive method since it is based on a simple core algorithm which in turn makes it easy to adapt to complex application scenarios. Moreover, the base algorithm of the LBM can easily be extended to capture additional physical effects. Consequently, this method is being used as a universal tool in a rapidly increasing number of research projects. However, the flexibility of the LBM comes

* Corresponding author; e-mail: hasansajadi@gmail.com

at a high price in terms of computational cost which routinely requires the use of parallel supercomputers [9-15].

To model the flow LES in a lattice Boltzmann scheme for discretizing the Navier-Stokes equations was used in previous works. LBM demonstrates that it can be a powerful method for simulating of turbulence flows [16-20]. The implementation of a LBM procedure is much easier for turbulence flows than that of traditional CFD methods. Meanwhile, it is more popular due to the balance between accuracy and efficiency. Because of these advantages, it was applied at past works regularly. Yu *et al*. [21] considered the application of multiple-relaxation-time (MRT) LBE for LES of turbulent flows. They demonstrated that MRT-LBE is a potentially viable tool for LES of turbulence. Fernandino *et al*. [22] investigated LES of turbulent open duct flow are performed using the LBM in conjunction with the Smagorinsky sub-grid scale (SGS) model. Whereas they found that the LBM simulation results are in good qualitative agreement with the experiments. Chen [23] proposed a novel and simple large-eddy-based LBM to simulate 2-D turbulence. He showed that the model is efficient, stable, and simple for 2-D turbulence simulation. The LBM with a forcing scheme is used to simulate homogeneous isotropic turbulence by Kareem *et al*. [24]. They received that the turbulence characteristics of the flow are similar to those obtained in studies by the spectral method regardless of which model is used. Recently Sajjadi *et al*. [25] studied numerical analysis of turbulent natural convection in square cavity using LES in LBM. They exhibited this method is in acceptable agreement with other verifications of such a flow.

The main aim of this investigation is to present large eddy turbulence model by LBM with a clear and simple statement. Thus natural convection turbulence flow in tall enclosures is investigated in a wide range of Rayleigh numbers. Although natural convection turbulence flow in confined convection is not only a topic for analysis but is comparable for numerical and experimental investigations. The first LBM is considered briefly and then large eddy was applied in LBM whereas theirs equations is expressed completely. Finally results of this study are compared with an experimental research.

Numerical method

Problem statement

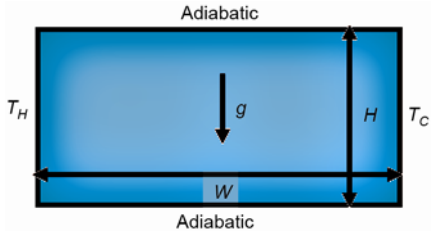

Figure 1. Geometry of the present study

The geometry of the present problem is shown in fig.1. It displays a 2-D enclosure with height of H and width of W. The temperatures of the two sidewalls of the cavity are maintained at T_H and T_C, where T_C has been considered as the reference condition. The top and the bottom horizontal walls have been considered to be adiabatic *i. e*., non-conducting and impermeable to mass transfer. The density variation in the fluid is approximated by the standard Boussinesq model. The fluid is assumed to be Newtonian, incompressible and the laminar whereas Prandtl number equals to Pr = 0.71. Also it is assumed that Mach number is fixed at Ma = 0.1.

Lattice Boltzmann method

In this paper a square grid and D2Q9 model is used for both flow and temperature functions. By detachment of Navier-Stocks equations, governing equations for flow and temperature functions are:

– for the flow field:

$$f_i(x + c_i\Delta t, t + \Delta t) - f_i(x,t) = \frac{1}{\tau_v}\left[f_i(x,t) - f_i^{eq}(x,t) \right] + \Delta t c_i F_i \tag{1}$$

– for the temperature field:

$$g_i(x + c_i\Delta t, t + \Delta t) - g_i(x,t) = \frac{1}{\tau_c}\left[g_i(x,t) - g_i^{eq}(x,t) \right] \tag{2}$$

where c_i is the discrete particle velocity vector defined (fig. 2), Δt – the lattice time step which is set to unity, τ_v, and τ_c are the relaxation times for the flow and temperature fields, respectively, f_i^{eq}, and g_i^{eq} – the local equilibrium distribution functions that have an appropriately prescribed functional dependence on the local hydrodynamic properties which are calculated with eqs. (3) and (4) for flow and temperature fields, respectively. F_i is an external force term.

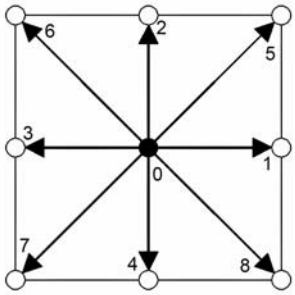

Figure 2. The discrete velocity vectors for D2Q9

$$f_i^{eq}(x,t) = \omega_i \rho \left[1 + \frac{c_i u}{c_s^2} + \frac{1}{2}\frac{(c_i u)^2}{c_s^4} - \frac{1}{2}\frac{uu}{c_s^2} \right] \tag{3}$$

$$g_i^{eq} = \omega_i T \left[1 + \frac{c_i u}{c_s^2} \right] \tag{4}$$

For the 2-D case, applying third-order Gauss-Hermite quadrature leads to the D2Q9 model with the following discrete velocities c_i, where $i = 1 \ldots 8$:

$$c_i = \begin{cases} 0 & i = 0 \\ c\left\{ \cos\left[(i-1)\frac{\pi}{2} \right], \quad \sin\left[(i-1)\frac{\pi}{2} \right] \right\} & i = 1\text{-}4 \\ c\sqrt{2}\left\{ \cos\left[(i-5)\frac{\pi}{2} + \frac{\pi}{4} \right], \quad \sin\left[(i-5)\frac{\pi}{2} + \frac{\pi}{4} \right] \right\} & i = 5\text{-}8 \end{cases} \tag{5}$$

where $\omega_0 = 4/9$, $\omega_{1-4} = 1/9$, $\omega_{5-9} = 1/36$, and $c = (3RT_m)^{-1/2}$ (to improve numerical stability T_m is the mean value of temperature for the calculation of c).

Using a Chapman-Enskog expansion, the Navier-Stokes equations can be recovered with the described model. The kinematic viscosity υ and the thermal diffusivity α are then related to the relaxation times by:

$$\vartheta = \left(\tau_v - \frac{1}{2} \right) c_s^2 \Delta t \quad \text{and} \quad \alpha = \left(\tau_c - \frac{1}{2} \right) c_s^2 \Delta t \tag{6}$$

where c_s is the speed of sound and equals to $c/3^{1/2}$.

In the simulation the Boussinessq approximation is applied to the buoyancy force term. In that case, the external force F appearing in eq. (1) is:

$$F_i = 3\omega_i g_y \beta \Delta T \tag{7}$$

where g_y, β, and ΔT are gravitational acceleration, thermal expansion coefficient, and temperature difference, respectively.

Finally, the macroscopic variables ρ, u, and T can be calculated:

$$\text{– flow density: } \rho = \sum_i f_i \tag{8}$$

$$\text{– momentum: } \rho u_j = \sum_i f_i c_{ij} \tag{9}$$

$$\text{– temperature: } T = \sum_i g_i \tag{10}$$

Large eddy simulation method

In this model the main aim is obtaining ν_t and $\alpha_t = \nu_t/\mathrm{Pr}_t$ where Pr_t is the turbulent Prandtl number which is assumed to be 0.5. In order to evaluate ν_t we perform:

$$\nu_t = (C\Delta)^2 \left(\left|\overline{S}\right|^2 + \frac{\mathrm{Pr}}{\mathrm{Pr}_t} \nabla T \frac{\vec{g}}{|\vec{g}|} \right)^{1/2} \tag{11}$$

where C is considered the Smagorinsky constant and in this paper it is assumed as 0.1 [17] and is gained from $\Delta = [(\Delta x)^2 + (\Delta y)^2]^{-1/2}$, where Δx and Δy are the grid extents in x- and y-directions.

For $\left|\overline{S}\right|$ we have:

$$\left|\overline{S}\right| = \sqrt{2\overline{S}_{\alpha\beta}\overline{S}_{\alpha\beta}} \tag{12}$$

$$\overline{S}_{\alpha\beta} = \frac{\partial_\alpha \overline{u}_\beta + \partial_\beta \overline{u}_\alpha}{2} \tag{13}$$

Lattice Boltzmann method based on large eddy simulation model

Large eddy model can be easily incorporated in LBM if we apply the following influence of ν_t on relaxation time [18-20].

$$\nu_{\text{total}} = c_s^2(\tau_m - 0.5) = \nu_0 + \nu_t \tag{14}$$

where ν_{total} and ν_0 are total viscosity and initial viscosity, respectively.

$$\tau_m = \frac{(\nu_0 + \nu_t)}{c_s^2} + 0.5 = \frac{\nu_0}{c_s^2} + 0.5 + \frac{\nu_t}{c_s^2} = \tau_0 + \frac{\nu_t}{c_s^2} \tag{15}$$

To obtain ν_t in LBM we have:

$$\left|\overline{S}\right| = \frac{3}{2\tau_m}|Q| \tag{16}$$

$$Q = \sum_{i=0}^{8} e_{i\alpha} e_{i\beta} (f_i - f_i^{eq}) \tag{17}$$

If we put $\left|\overline{S}\right|$ in eq. (11):

$$\nu_t = (C\Delta)^2 \sqrt{\frac{9}{4\tau_m^2}|Q|^2 + \frac{\mathrm{Pr}}{\mathrm{Pr}_t}\nabla T \frac{\vec{g}}{|\vec{g}|}} \tag{18}$$

and if we substitute the eq. (18) in eq. (15):

$$\tau_{\text{total}} = \tau_0 + \frac{(C\Delta)^2 \sqrt{\frac{9}{4\tau_m^2}|Q|^2 + \frac{\mathrm{Pr}}{\mathrm{Pr}_t}\nabla T \frac{\vec{g}}{|\vec{g}|}}}{c_s^2} \tag{19}$$

To obtain relaxation time in temperature function equation we have:

$$\tau_h = \tau_{D0} + \frac{\alpha_t}{c_s^2} = \tau_{D0} + \frac{\nu_t / \mathrm{Pr}_t}{c_s^2} \tag{20}$$

where $\tau_{D0} = (\alpha_0 / c_s^2) + 0.5$.

Substituting new relaxation time in eqs. (1) and (2) yields to Lattice Boltzmann equations based on large eddy model.

Boundary conditions

Flow

Implementation of boundary conditions is very important for the simulation. The unknown distribution functions pointing to the fluid zone at the boundaries nodes must be specified. Concerning the no-slip boundary condition, bounce back boundary condition is used on the solid boundaries. For instance the unknown density distribution functions at the boundary east can be determined by the conditions:

$$f_{6,n} = f_{8,n}, \quad f_{7,n} = f_{5,n}, \quad f_{3,n} = f_{1,n} \tag{21}$$

where n is the lattice on the boundary.

Temperature

The north and south of the boundaries are adiabatic then bounce back boundary condition is used on them. Temperature at the west and east wall are known, in the west wall $T_{\mathrm{H}} = 1.0$. Since we are using D2Q9, the unknowns distribution function are g_1, g_5, and g_8 at west wall which are evaluated as:

$$g_1 = T_H(\omega_1 + \omega_3) - g_3, \quad g_5 = T_H(\omega_5 + \omega_7) - g_7, \quad g_8 = T_H(\omega_8 + \omega_6) - g_6 \tag{22abc}$$

Nusselt number Nu is one of the most important dimensionless parameters in describing the convective heat transport. The local Nusselt number and the average value at the hot and cold walls are calculated as:

$$\mathrm{Nu}_y = -\frac{H}{\Delta T}\frac{\partial T}{\partial x} \tag{23}$$

$$\mathrm{Nu}_{\mathrm{avg}} = \frac{1}{H}\int_0^H \mathrm{Nu}_y \mathrm{d}y \tag{24}$$

Finally, the following criterion to check for the steady-state solution was used:

$$Error = \max\left|T^{n+1} - T^n\right| \le 10^{-5} \tag{25}$$

Code validation

Table 1. Comparison of mean Nu with previous works

Ra number	Mesh	Mean Nu (this work)	Mean Nu [2]	Mean Nu [16]
10^7	256 × 256	17.2	–	16.8
10^8	512 × 512	31.2	32.3	30.5
10^9	1024 × 1024	58.1	60.1	57.4

The tall enclosures were investigated at different Rayleigh numbers of 10^7, 10^8, and 10^9, with three various aspect ratios of A = 0.5, 1, and 2. Turbulent natural convection with LES method were conducted in this paper. An extensive mesh testing procedure was conducted to guarantee a grid independent solution. Finally numbers of the lattices for different Rayleigh numbers and average Nusselt number comparison of present results with two previous studies were displayed at tab. 1.

The present numerical method was validated with experimental researches of Ampofo and Karayiannis [3]. A comparison with velocity at the middle section of the cavity and local Nusselt number on the hot wall were considered with experimental results of Ampofo and Karayiannis [3] in fig. 3. Table 1 shows the comparison of the average Nusselt numbers for different Rayleigh numbers between present results and finds of Barakos*et al* [2], Dixit [16] as cavity was filled by air with Pr = 0.71. Clearly it is seen that the results match previous works. Furthermore this table demonstrates needful various meshes to utilize for different Rayleigh numbers. These comparisons show that the present study has a good agreement with previous studies.

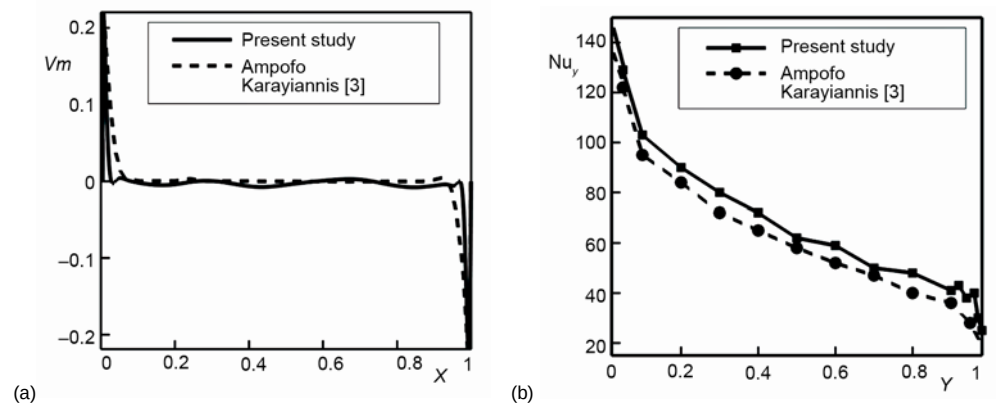

Figure 3. Comparison of the velocity on the axial midline (a) and local Nusselt number (b) between the present results and numerical results by Ampofo and Karayiannis [3] (Ra = $1.58 \cdot 10^9$)

Results and discussions

Figure 4 shows the contour maps for the isotherms at various Rayleigh numbers and different enclosure aspect ratios. When Rayleigh number increases, the convection process in

the isotherms for various aspect ratios augments. The process is obvious whereas the isotherm of $T = 0.9$ moves from the upper left corner of the enclosure at Ra = 10^7 toward the cold wall of the enclosure at Ra = 10^9. The isotherms are vibrant at Ra = 10^7, but this manner changes to a steady-state at higher Rayleigh numbers. The increment of the aspect ratios causes the movement of the isotherms from the hot wall to the cold wall declines. This phenomenon is quite obvious at Ra = 10^7 whereas both isotherms of $T = 0.8$ and 0.2 at $A = 2$ set between two vertical walls and move towards the horizontal walls.

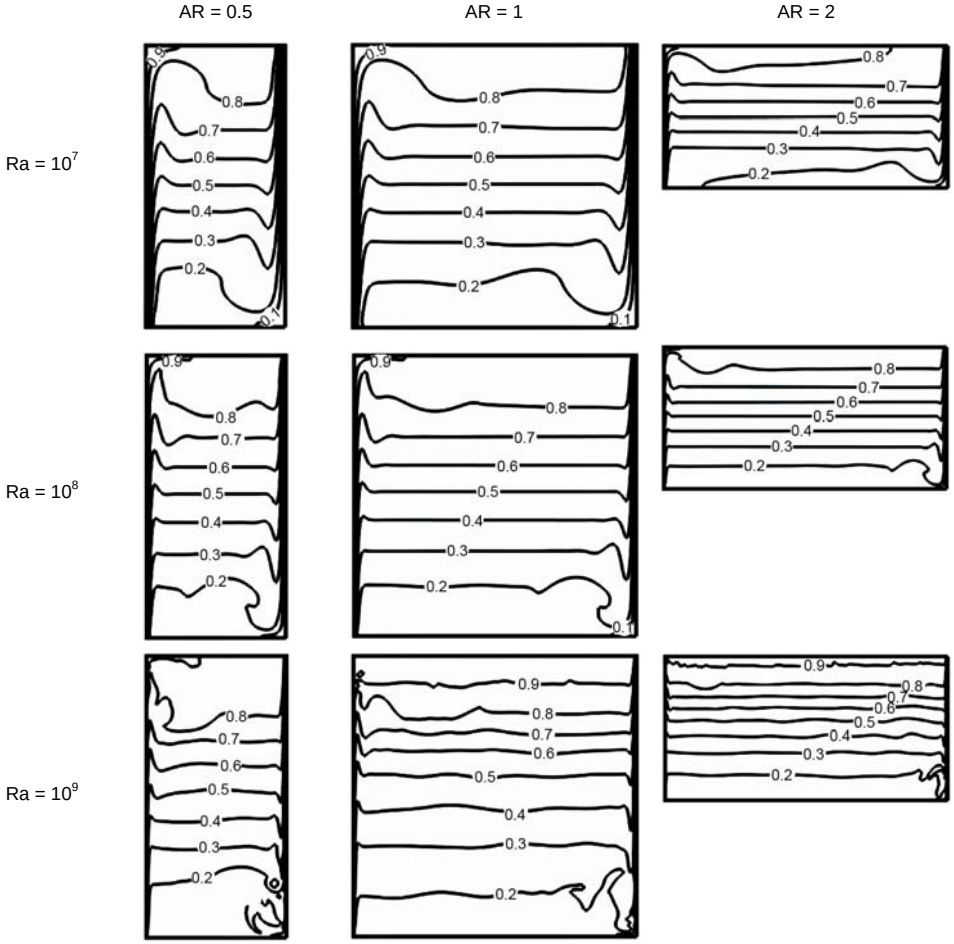

Figure 4. Comparison of the isotherms at various aspect ratios and Rayleigh numbers

Figure 5 displays the streamlines at various Rayleigh numbers and different enclosure aspect ratios. The streamlines have a regular process until Ra = 10^8 and the changes are marginal into the streamlines, but at Ra = 10^9 the form of the streamlines change completely and they revolve around some different vortexes at this Rayleigh number. The maximum values of the streamlines behave erratically for different aspect ratios and Rayleigh numbers. The maximum values of the streamlines decrease from Ra = 10^7 to 10^8 while the value at Ra = 10^9 jumps to a higher amount of Ra = 10^7 suddenly. Moreover, the maximum values of the streamlines have the most their values at AR = 1 among different aspect ratios and Rayleigh

numbers. It is clear that turbulence in the enclosures at AR = 2 is less than other two aspect ratios for various Rayleigh numbers and their trend is smooth so the maximum values of the streamlines has the least their values at AR = 2.

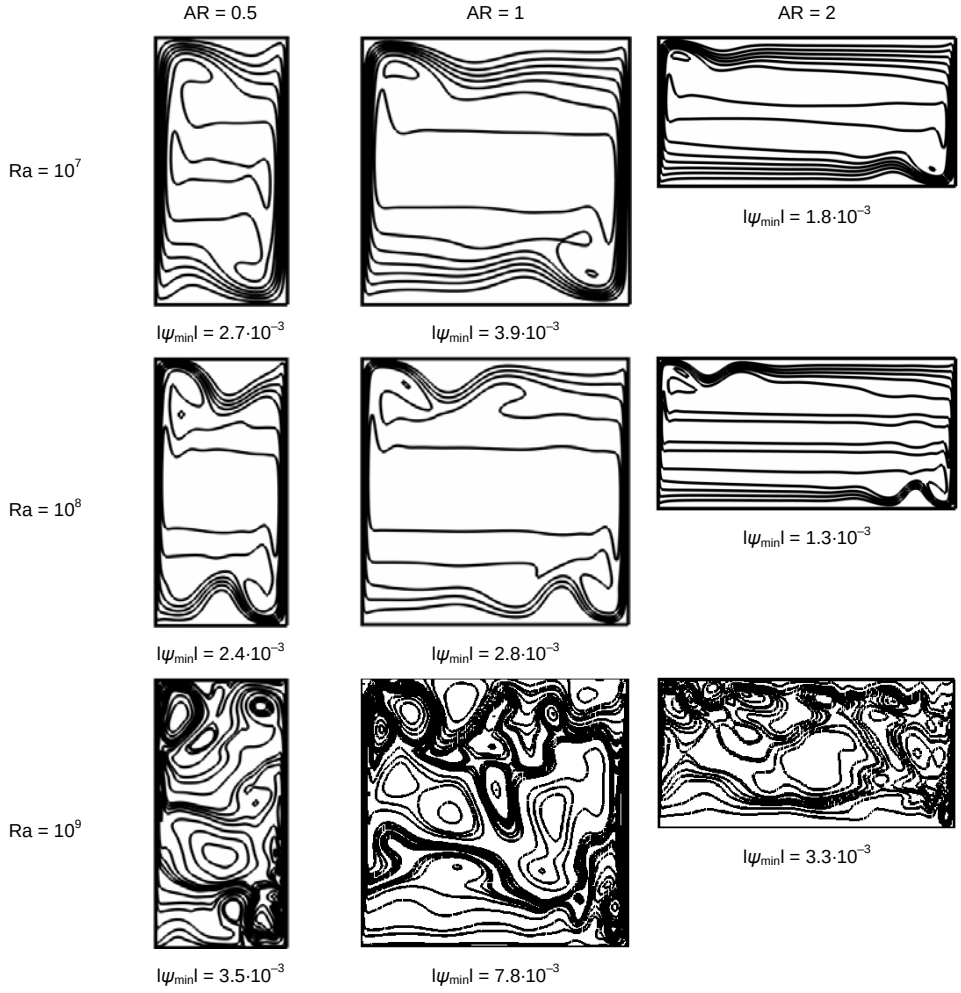

Figure 5. Comparison of the streamlines at various aspect ratios and Rayleigh numbers

Figure 6 illustrates the distribution of the local Nusselt number on the hot wall for different aspect ratios and Rayleigh numbers. The trend of the local Nusselt number is the same for various Rayleigh number and just their values increase by the augmentation of Rayleigh number at various aspect ratios. The effect of aspect ratios on the local Nusselt number is negligible and the difference is considerable at $Y/H > 0.8$ for AR = 2,1, and $Y/H > 0.4$ for AR = 0.5, whereas the isotherm of $T = 0.9$ have an important influence on the isotherms.

Figure 7 demonstrates the values of the vertical velocity on the axial midline for different Rayleigh numbers and aspect ratios. When Rayleigh enhances, the sudden changes near the vertical walls happen in a closer place to the walls. The maximum and minimum of the vertical velocity on the axial midline which are close to vertical walls augments with the growth of Rayleigh numbers. On the other hand, when the aspect ratio increases, the vertical

velocity on the axial midline vibrates at Ra = 10^9 and the increment of the aspect ratio increase the amplitudes values of the vibrations.

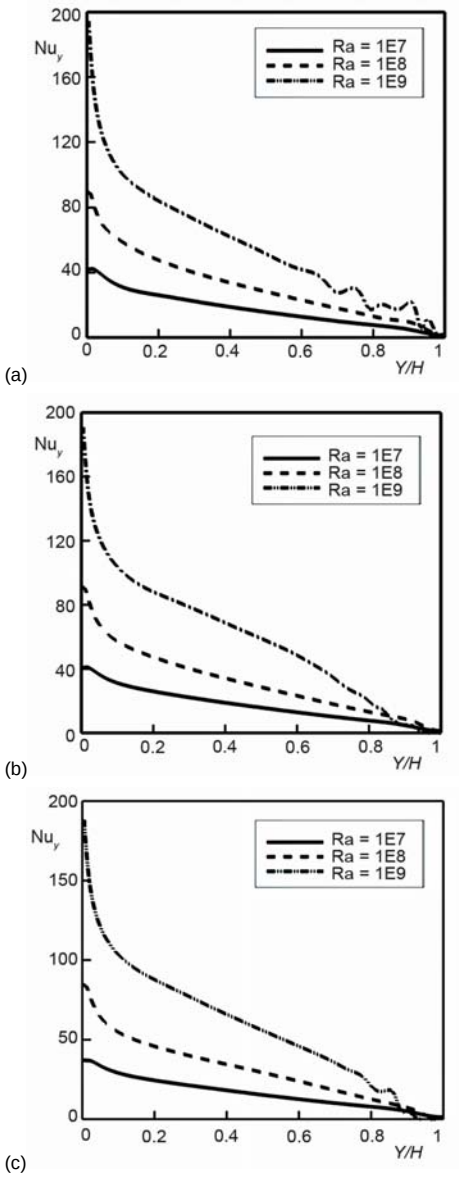

Figure 6. Values of the local Nusselt number for different aspect ratios (a) AR = 0.5, (b) AR = 1, and (c) AR = 2

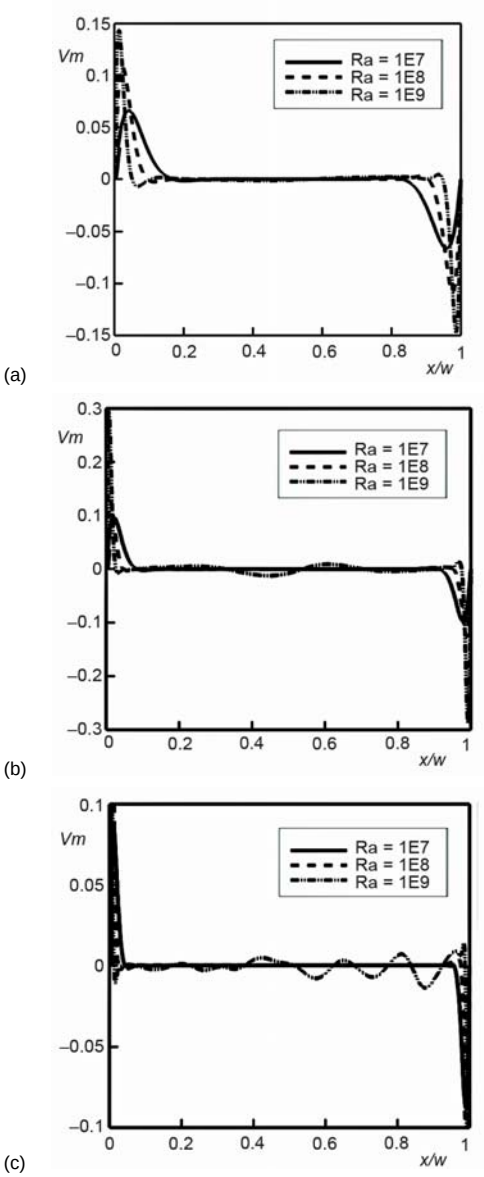

Figure 7. Values or the vertical velocity on the axial midline for different Rayleigh numbers and aspect ratios (a) AR = 0.5, (b) AR = 1, and (c) AR = 2

Figure 8 exhibits the values of the temperature on the axial midline for different Rayleigh numbers and aspect ratios. It is clear that the value declines with the augmentation of Rayleigh numbers whereas this fall is marginal at AR = 0.5 and has the greatest value at

AR = 2. When the aspect ratio increases, the values change near the vertical walls gets less and smooth.

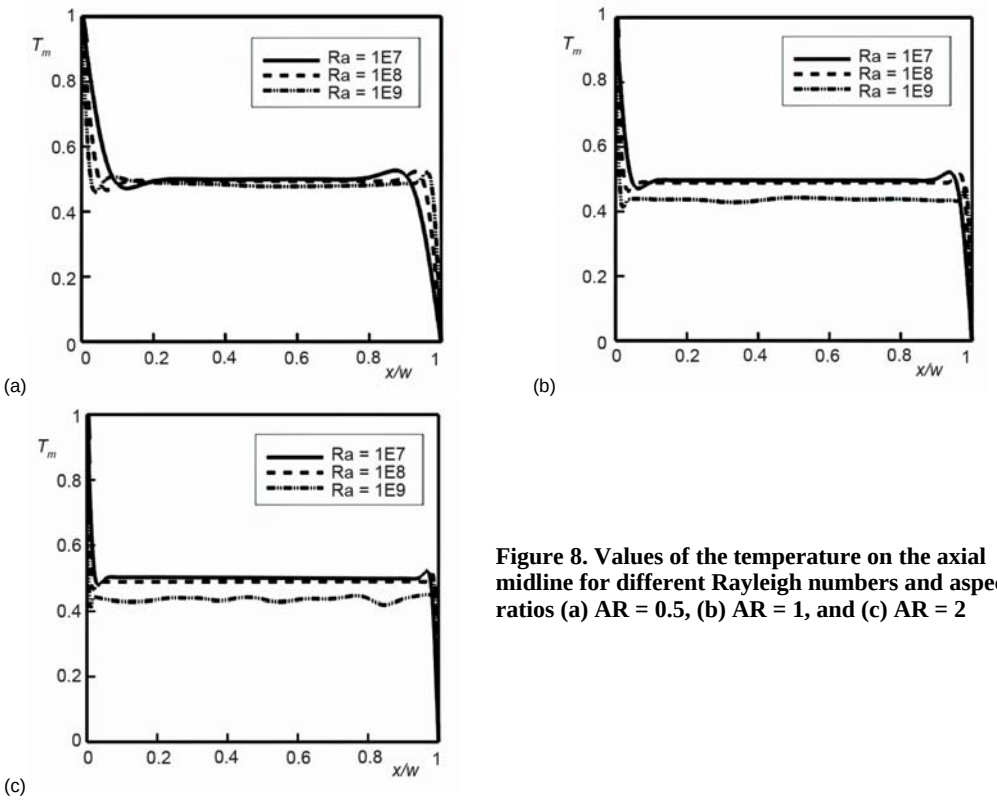

Figure 8. Values of the temperature on the axial midline for different Rayleigh numbers and aspect ratios (a) AR = 0.5, (b) AR = 1, and (c) AR = 2

Figure 9 indicates the value of the average Nusselt number and the normalized average Nusselt number. The figure shows that the average Nusselt number decreases with the increment of the aspect ratios at various Rayleigh numbers. The values of the normalized average Nusselt number demonstrates that the greatest effect of aspect ratios happens at Ra = 10^7 while the least effect observes at Ra = 10^8.

Conclusions

Turbulent natural convection in tall enclosures which are filled with air with Pr = 0.71 has been conducted numerically by LBM. This study has been carried out for the pertinent parameters in the following ranges: the Rayleigh number of base fluid (Ra = 10^7-10^9), aspect ratios (AR) of the enclosure (AR = 0.5-2), and some conclusions were summarized.

- A proper validation with previous numerical investigations demonstrates that LBM is an appropriate method for turbulent flows problems.
- Generally, the decrease in the aspect ratios and the Rayleigh numbers enhancement result in the augmentation of heat transfer.
- The form of the streamlines changes completely when Rayleigh number increases from Ra = 10^8 to 10^9.

The most effect of the aspect ratio changes is observed at Ra = 10^7 among considered Rayleigh numbers.

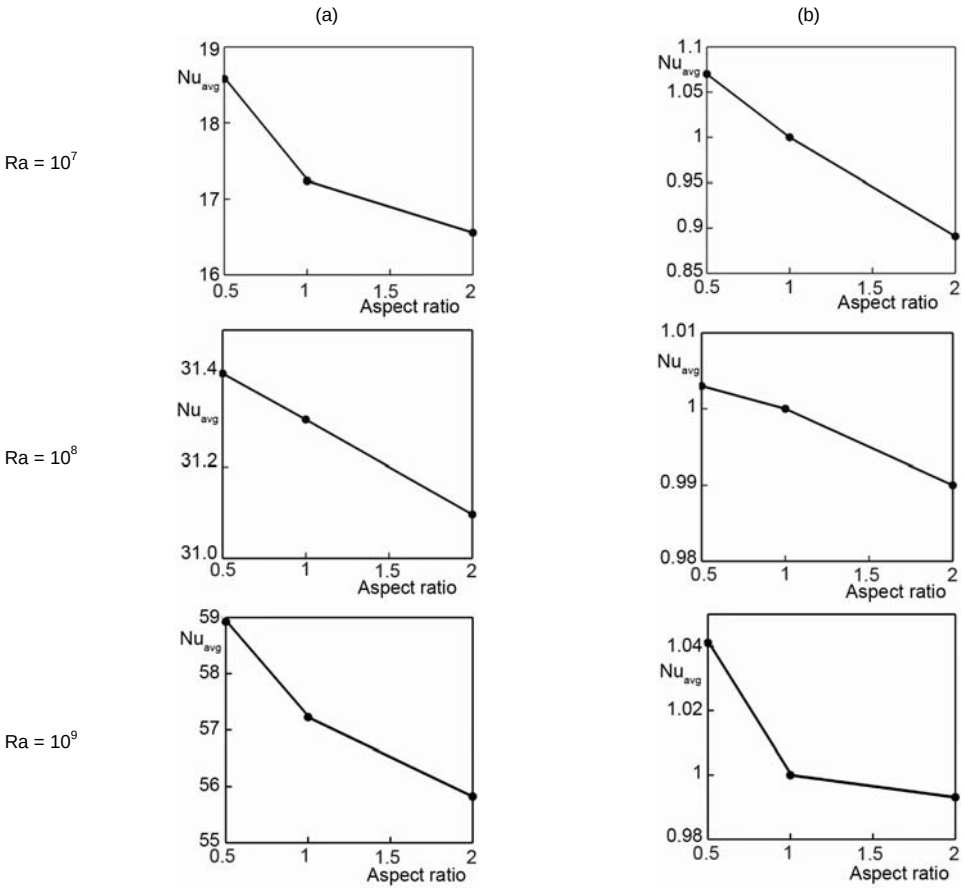

Figure 9. Average Nusselt number (a) and (b) normalized Nusselt number distributions on the hot wall at different aspect ratios and Rayleigh numbers

Nomenclature

c – lattice speed
c_i – discrete particle speeds
c_p – specific heat at constant pressure
F – external forces
f – density distribution functions
f^{eq} – equilibrium density distribution functions
g – internal energy distribution functions
g^{eq} – equilibrium internal energy distribution functions
g_y – gravity
H – cavity height
Nu – Nusselt number
Pr – Prandtl number
R – constant of the gases
Ra – Rayleigh number
$\overline{S}_{\alpha\beta}$ – strain rate tensor
T – temperature
Δt – time increment
Δx – lattice spacing
x, y – Cartesian co-ordinates
V_m – vertical velocity on the axial fields
W – cavity width

Greek symbols

μ – dynamic viscosity
ν – kinematic viscosity
ρ – density
τ_c – relaxation time for temperature
τ_v – relaxation time for flow
ω_i – weighted factor in direction i

Subscripts

avg – average
C – cold
f – fluid
H – hot
t – turbulence

Reference

[1] Frisch, U., *Turbulence: The Legacy of A. N. Kolmogorov,* Cambridge University Press, New York, 1995
[2] Barakos, G., *et al.*, Natural Convection Flow in a Square Cavity Revisited: Laminar and Turbulent Models with Wall Function, *Int. J. Numerical Method in Fluids, 18* (1994), 7, pp. 695-719
[3] Ampofo, F., Karayiannis, T. G., Experimental Benchmark Data for Turbulent Natural Convection in an Air Filled Square Cavity, *Int. J. Heat and Mass Transfer, 46* (2003), 19, pp. 3551-3572
[4] Smagorinsky, J., General Circulation Experiments with the Primitive Equations, *Mon. Wea. Rev, 91* (1963), 3, pp. 99-164
[5] Lilly, D., *On the Application of the Eddy Viscosity Concept in the Inertial Sub-Range of Turbulence*, National Center for Atmospheric Research, Boulder, Col., USA, 1966
[6] Deardorff, J., A Numerical Study of Three-Dimensional Channel Flow at Large Reynolds Numbers, *J. Fluid Mech., 41* (1970), 2, pp. 453-480
[7] Schumann, U., Subgrid Scale Model for Finite Difference Simulations of Turbulent Flows in Plane Channels and Annuli, *J. Comput. Phys., 18* (1975), 4, pp. 376-404
[8] Leonard, A., Energy Cascade in Large-Eddy Simulations of Turbulent Fluids Flows, *Adv. Geo. Phys., 18* (1974), A, pp. 237-248
[9] Succi, S., *The Lattice Boltzmann Equation for Fluid Dynamics and Beyond*, Clarendon Press, Oxford, UK, 2001
[10] Sajjadi, H., *et al.*, Lattice Boltzmann Simulation of MHD Mixed Convection in Two Sided Lid-Driven Square Cavity, *Heat Transfer-Asian Research, 41* (2012) 2, pp. 179-195
[11] Mohamad, A. A., Kuzmin, A., A Critical Evaluation of Force Term in Lattice Boltzmann Method, Natural Convection Problem, *Int. J. Heat and Mass Transfer, 53* (2010), 5-6, pp. 990-996
[12] Sajjadi, H., *et al.*, Lattice Boltzmann Simulation of Turbulent Natural Convection in Tall Enclosures Using Cu/Water Nanofluid, *Num. Heat Transfer, Part A, 62* (2012), 6, pp. 512-530
[13] Sajjadi, H., *et al.*, Lattice Boltzmann Simulation of Natural Convection in an Inclined Heated Cavity Partially Using Cu/Water Nanofluid, *Int. J. Fluid Mech. Res., 39* (2012), 4, pp. 348-372
[14] Kefayati, GH. R., *et al.*, Lattice Boltzmann Simulation of Natural Convection in Tall Enclosures Using Water/ SiO_2 Nanofluid", *Int. Comm. Heat and Mass Transfer, 38* (2011), 6, pp. 798-805
[15] Kefayati, GH. R., *et al.*, Lattice Boltzmann Simulation of Natural Convection in an Open Enclosure Subjugated to Water/Copper Nanofluid", *Int. J. Therm. Sci., 52* (2012), 1, pp. 91-101
[16] Dixit, H. N., Babu, V., Simulation of High Rayleigh Number Natural Convection in a Square Cavity Using the Lattice Boltzmann Method, *Int. J. Heat and Mass Transfer, 46* (2006), 4, pp. 727-739
[17] Horvat, A., *et al.*, Two-Dimensional Large-Eddy Simulation of Turbulent Natural Convection due to Internal Heat Generation, *Int. J. Heat and Mass Transfer, 44* (2001), 21, pp. 3985-3995
[18] Hou, S., *et al.*, A Lattice Boltzmann Subgrid Model for High Reynolds Number Flows, *Fields Inst. Comm., 6* (1996), pp. 151-166
[19] Teixeira, C. M., Incorporation Turbulence Models into the Lattice-Boltzmann Method, *Int. J. Mod. Phys. C, 9* (1998), 8, pp. 1159-1175
[20] Krafczyk, M., *et al.*, Large-Eddy Simulations with a Multiple-Relaxation-Time LBE Model, *Int. J. Mod. Phys. B, 17* (2003), 1-2, pp. 33-39
[21] Yu, H., *et al.*, LES of Turbulent Square Jet Flow Using an MRT Lattice Boltzmann Model, *Comp. & Flu., 35* (2006), 8-9, pp. 957-965
[22] Fernandino, M., *et al.*, Large Eddy Simulation of Turbulent Open Duct Flow Using a Lattice Boltzmann Approach, *Math. Comp. in Simulation, 79* (2009), 5, pp. 1520-1526
[23] Chen, S., A Large-Eddy-Based Lattice Boltzmann Model for Turbulent Flow Simulation, *App. Math. Comp., 215* (2009), 2, pp. 591-598
[24] Kareem, W. A., *et al.*, Lattice Boltzmann Simulations of Homogeneous Isotropic Turbulence, *Comp. Math. With Appl., 58* (2009), 5, pp. 1055-1061
[25] Sajjadi, H., *et al.*, Numerical Analysis of Turbulent Natural Convection in Square Cavity Using Large-Eddy Simulation in Lattice Boltzmann Method, *IR. J. Sci. & Tech. Tran. B/Eng., 35* (2011), M2, pp. 133-142

Paper submitted: January 5, 2012
Paper revised: January 28, 2012
Paper accepted: June 5, 2013